Bandwidth Enhancement of Substrate Integrated Waveguide Tunnels by Longitudinal Resonances

Alonso Corona-Chavez[1,2] and Tatsuo Itoh[1]

[1]Electrical Engineering Department, UCLA, Los Angeles, CA, 90095
[2]National Institute of Astrophysics, Optics and Electronics (INAOE), Puebla, Mexico, 72000

***Abstract* — A new method to achieve wide pass-band characteristics on Substrate Integrated Waveguide (SIW) tunnel section is presented. It will be shown that three in-band longitudinal resonant-modes can be excited from the waveguide-feed interaction due to the frequency dispersive nature of the effective permittivity in a waveguide. Such modes correspond to the Epsilon Near Zero (ENZ) mode, a half-wavelength mode, and one-wavelength mode. In this paper theoretical and experimental results are presented to validate the concept.**

***Index Terms* — Substrate Integrated Waveguide, Epsilon Near Zero, Waveguides, Resonant tunneling devices.**

I. Introduction

Substrate Integrated Waveguides (SIW) support TE_{10} propagation mode which has an intrinsic high pass characteristic [1]. However, for wide pass-band characteristics electromagnetic band gap structures or notch resonators have been added to the SIW [2, 3, 4].

In this work a new technique to obtain wide pass-band characteristics on SIW tunnel section is presented. This method relies on the excitation of three in-band resonant-modes that arise from the waveguide-feed interaction. Such resonant modes correspond to the Epsilon Near Zero (ENZ) mode (with infinite wavelength) [5], a half-wavelength mode and one-wavelength mode. To excite these resonant modes a modified tapered feed is used.

An SIW with an ε_r substrate operated at the fundamental TE_{10} mode has an effective permittivity described by (1) [6].

$$\frac{\varepsilon_{eff}}{\varepsilon_0} = \varepsilon_r \varepsilon_0 - \frac{c^2}{4f^2 W_g{}^2} \qquad (1)$$

where c is the speed of light in vacuum, f is the operation frequency and W_g is the waveguide width. From the equation it is clear that the effective permittivity is negative below cutoff ($\varepsilon_{eff} < 1$). Above cutoff it is positive ($\varepsilon_{eff} > 0$), and at cutoff, ε_{eff}=0. This implies that at cutoff the phase constant is zero ($\beta = 0$) which gives rise to an infinite guided wavelength [5]. As a result, the structure is perfectly matched at this frequency. This phenomenon, often called tunneling, has been previously reported for antenna feeds [7], for matched waveguide-bends [8], and for narrow waveguide tunnels [9]. The operational bandwidth of these tunnels is generally very narrow since only one frequency is transmitted. Although the TE_{10} waveguide itself has a high pass characteristic, we try to create a wide band-pass characteristic in place of an extremely narrow bandwidth of the ENZ.

In order to create three in-band resonant modes the feed-tunnel interaction is used. The first mode corresponds to the ENZ tunnel.

The second resonant mode is excited only on the feed lines since the electrical length of the tunnel becomes negligibly small. This effect occurs for frequencies where the guided wavelength is much larger than the free ε_r medium wavelength.

Finally, a third resonant mode is excited on the feed lines and the tunnel, which happens for frequencies when the tunnel acts as a distributed element. This takes place when the guided wavelength is similar to the free medium wavelength.

For filter applications, sharp skirt roll-offs are required. Therefore, two quarter-wavelength decoupling resonators were added to the circuit to generate transmission zeroes at the edges of the passband.

In this paper a structure is presented with 75% bandwidth. Good agreement between simulation and experimental results is achieved.

II. ENZ Waveguide structure

Fig. 1a shows the proposed structure which consists of an SIW tunnel fed by a modified taper feed, where a window is cut with dimensions a and b. W_g is the width of the tunnel, L_g is its length, L_f is the length of the taper and W_f is the width of the taper. For a TE_{10} mode, the SIW tunnel width can be obtained by (2).

$$W_g = \frac{c}{2 f_1 \sqrt{\varepsilon_r}} \qquad (2)$$

Where f_1 is the cutoff frequency, c is the speed of light and ε_r is the relative permittivity. For our case we chose ε_r =2.2 and f_1= 2.5GHz, which gives W_g= 40mm. The other dimensions are a= 14mm, b= 4mm, L_g= L_f= 10mm, and W_f= 16mm. The substrate height is h=0.5mm. The tunnel has a phase constant (β_g) given by (3).

$$\beta_g = \sqrt{k^2 - \left(\frac{\pi}{W_t}\right)^2} \tag{3}$$

where $k = 2\pi \cdot f\sqrt{\varepsilon_r \varepsilon_o \mu_o}$ is the phase constant on a medium with permittivity ε_r . The guided wavelength is $\lambda_g=2\pi/\ \beta_g$ and the ε_r-medium wavelength is $\lambda=2\pi/\ k$. From here it can be seen that for β_g=0, $\lambda_g \to \infty$ (see Fig. 2).

When the structure is loaded with the modified taper, a slight frequency shift of the tunneling frequency occurs. The taper is a wide but short structure (its length is about λ/10 for f_1). Hence it has a strong capacitive contribution. By analogy from (2), an increase in the capacitance to ground results in an effective increase in permittivity (ε). A full wave simulation [11] of the structure was performed and the results plotted in Fig. 3 showing the effective ENZ tunneling frequency at about 2.1 GHz. Fig. 1b shows the simulated E-Field distribution at the tunneling frequency where a constant field is observed hence confirming the tunneling effect with infinite wavelength.

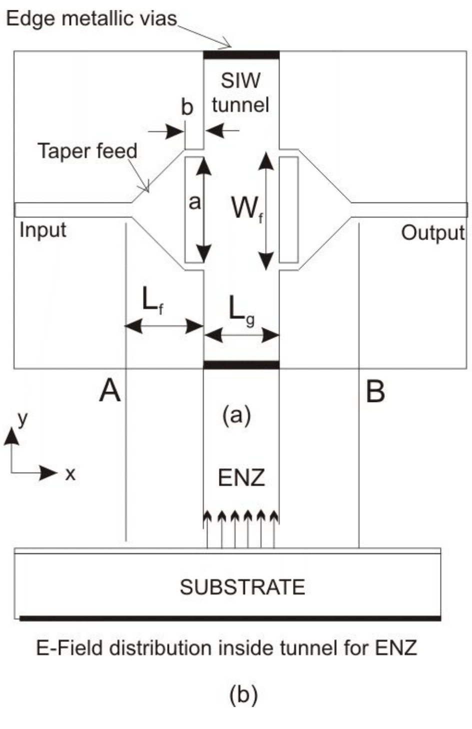

Fig. 1. (a) Top view of SIW structure with modified taper. (b) E-Field distribution inside the tunnel for ENZ.

An equivalent circuit of the structure is depicted in Fig. 4. The circuit can be seen as a feed transmission line with two short circuited stubs which represent the tunnel section. Since the length ($W_g/2$) of the stubs is λ/4 at the 2.5GHz cutoff (2), their input impedance Z_{INS} is infinite ($Z_{INS} = j \cdot Z_{IN} \tan(\beta \cdot W_g/2)$) therefore the tunnel is transparent to the propagating signal. Moreover, due to the static-like behavior in the x direction, their effective length L_{geff} can be taken infinitely small (or dimensionless) as shown in Fig. 4. Nevertheless, since the effective tunneling frequency is slightly shifted due to the capacitive loading of the feed, the length of the stubs ($W_g/2$) is about $\lambda/5$ at 2.1GHz. As it is well known, the input impedance of short-circuited stubs shorter than $\lambda/4$ is a positive imaginary number ($Z_S=32j$ in our case), consequently acting like inductors.

From Fig. 4, the T_1-T_2 ABCD matrix can be calculated from (4).

$$ABCD_{IN} = \begin{bmatrix} 1 & 0 \\ 1/Z_{CF} & 1 \end{bmatrix} \cdot \begin{bmatrix} 1 & 0 \\ 2/Z_{INS} & 1 \end{bmatrix} \cdot \begin{bmatrix} 1 & 0 \\ 1/Z_{CF} & 1 \end{bmatrix} \tag{4}$$

where Z_{CF} is the impedance of a capacitive element given by $Z_{CF}= 1/(j\ 2\pi f\ C_F)$ and $C_F = A\ \varepsilon_o\varepsilon_r/h$. A is the effective area of the taper feed. To calculate the reflection coefficient (5) can be used.

$$\Gamma_{IN} = \frac{A_{IN} + B_{IN}/Z_0 - C_{IN}Z_0 - D_{IN}}{A_{IN} + B_{IN}/Z_0 + C_{IN}Z_0 + D_{IN}} \tag{5}$$

where $Z_0=50\Omega$ is the line impedance beyond the feed. For our case $C_F \approx 2.5pF$ which gives a matched impedance condition at about 2.1GHz, in accordance with Fig. 3.

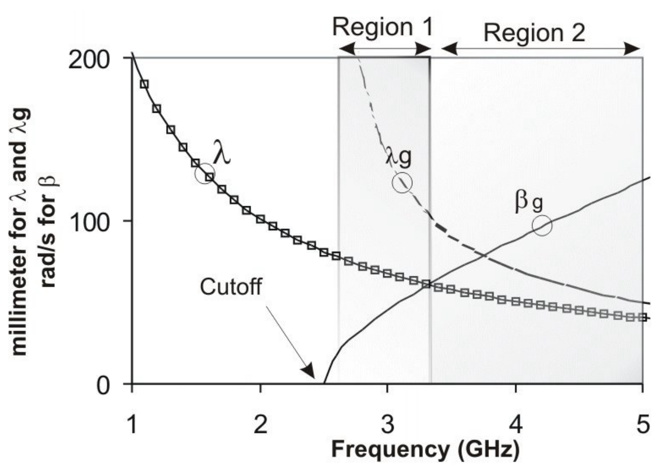

Fig. 2. Guided wavelength, phase constant (β) inside waveguide and ε_r-medium wavelength

III. 2[ND] AND 3[RD] IN-BAND RESONANCES

For frequencies above cutoff when $\beta_g \neq 0$ two regions can be defined as shown in Fig. 2. In Region 1, the guided wavelength is much larger than the wavelength in the ε_r medium (λ_g>>λ). In Region 2 the guided wavelength becomes comparable to the ε_r medium (λ ~=λ_g).

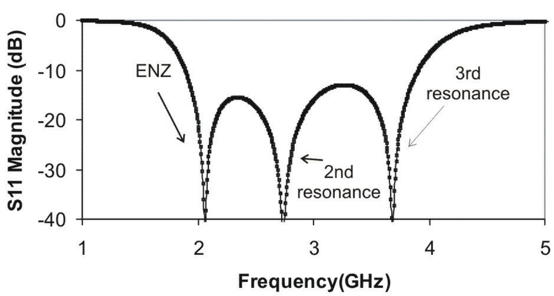

Fig. 3. Simulated S_{11} parameter of structure showing the three different resonances.

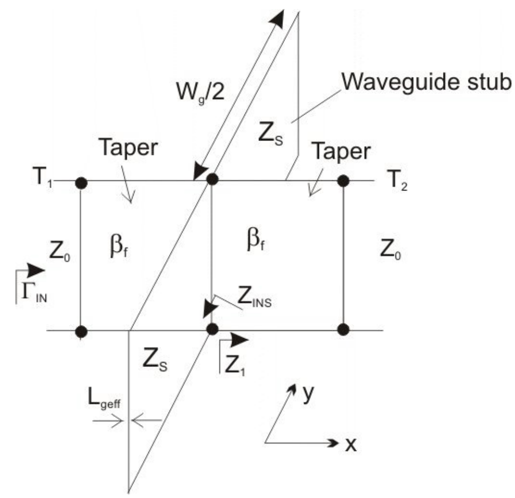

Fig. 4. Simplified model of structure.

For Region 1, (up to about 3.2GHz)), the electrical length of the tunnel is negligibly small ($\beta_g \cdot L_g << \lambda_g$). On the other hand, when the effective electrical length of the taper becomes about quarter wavelength ($\beta_f \cdot L_f \approx 90^\circ$), the structure supports a half-wave resonance, which is split between the two feeds. This is shown in Fig. 5a where the E-field distribution is depicted. It is clear that since the electrical length of the SIW is considerably small, there is no E-Field variation along it, whereas the half wavelength resonance is distributed on the tapers (which are about λ/4 each). In this case this happens at 2.8GHz. Fig. 3 shows the full wave simulation of the structure confirming the second longitudinal resonance at the given frequency.

For the third resonance, which occurs in Region 2 (Fig. 2) the guided wavelength is comparable to that of the ε_r medium (λ ~=λ_g). In addition, the electrical length of the waveguide is large enough to act like a distributed element. For this reason, when the electrical length of the whole structure approaches one wavelength, a third resonant mode is excited. In our case this occurs at 3.6GHz. The E-Field distribution is depicted in Fig. 5b showing that half of the wave is distributed along the tunnel and the other half is split between the input and output feeds. Finally, the simulation results confirm this finding as illustrated in Fig. 3 where the resonant mode at 3.6GHz is clearly seen.

IV. Notch Resonators

In order to improve the rejection characteristics at the lower and upper bands, two λ/4 notch resonators were added to the input and output of the structure. These resonators were designed at 1.5GHz and 4.5 GHz respectively. These resonators are decoupled from the transmission line by means of an interdigital capacitor from the input of the SIW tunnel. The final circuit is shown in Fig 6.

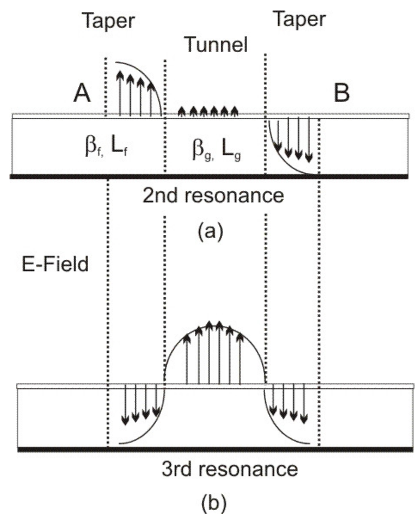

Fig. 5. (a) E-Field distribution for 2nd resonance, (b) E-Field distribution for 3rd resonance

V. Results

As discussed above, the width W_g defines the first ENZ resonance, whereas L_f , W_f and L_g define the second and third resonant modes. Different bandwidth behaviors can be obtained by optimizing these values.

The structure was realized on a RT 5880 Duroid substrate with ε_r=2.2 and h=0.5mm. The side walls of the tunnel were realized with copper tape. The measured and simulated results are compared in Fig. 7, clearly showing the three in-band resonant modes. The measured bandwidth is 70% and the simulated is 75%. The return losses are better than 17dB for simulation and experiment. The experimental insertion losses are below 1.5dB throughout the band. The simulation and experimental results show small differences due to manufacturing errors. However, reasonable agreement between simulation and experiment is achieved.

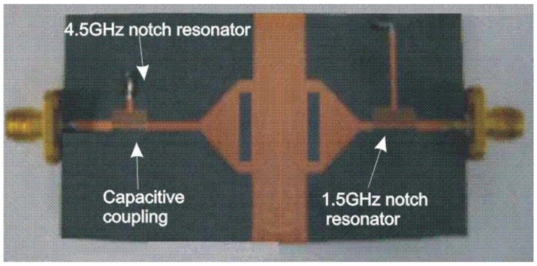

Fig. 6. Fabricated structure

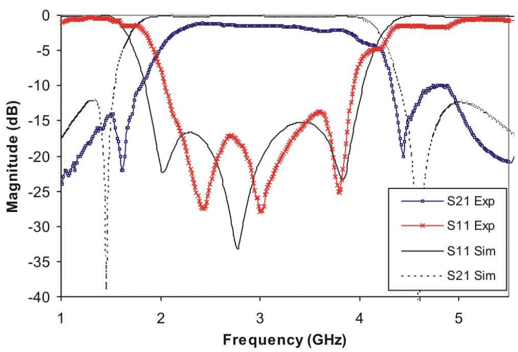

Fig. 7. Simulated and experimental responses of structure with wide pass-band response

VI. Conclusion

In this paper, a new technique to obtain wide pass bands has been demonstrated by means of exciting longitudinal resonances along an SIW tunnel. Such resonances correspond to ENZ, half wavelength and one wavelength. One tunnel was successfully built and tested showing reasonable agreement between simulated and measured results.

Acknowledgement

The authors wish to thank the Fulbright foundation for their sponsorship and Jim Sun from the Microwave Laboratory for his assistance in the fabrication process.

References

[1] Y. Cassivi, L. Perregrini, K. Wu and G. Conciauro, "Low-Cost and High-Q Millimeter-Wave Resonator Using Substrate Integrated Waveguide Technique", *European Microwave Conf.* 2002, Milan, Sept. 2002, vol. 2.

[2] Zhang-Cheng Hao, Wei Hong , Ji-Xin Chen, Xiao-Ping Chen, and Ke Wu, "CompactSuper-Wide Bandpass Substrate Integrated Waveguide (SIW) Filters," *IEEE Trans. Microw. Theory Tech*., vol. 53, no. 9, pp. 2968–2977, Sept 2005.

[3] Jing Wang, Wei Hong, Hong-Jun Tang, Yan Zhang, Yuan-Dan Dong, and Ke Wu, "UWB Bandpass Filter with Multiple Frequency Notched Bands," 2008 *IEEE MTT-S International Microwave Workshop Series on Art of Miniaturizing RF and Microwave Passive Components*, Chengdu, China December 2008, pp. 106-109.

[4] R. H. Gonzalez, D. V. Murthy, and A. Corona Chavez, "Ultra Wide Band Filter with Notch at WiMax using Epsilon Near Zero (ENZ) Methodology", *Asia Pacific Microwave Conference APMC 2009*, Singapore Dec 7-10, 2009.

[5] B. Edwards, A. Alù, M. E. Young, M. G. Silveirinha, and N. Engheta, "Experimental Verification of Epsilon-Near-Zero Metamaterial Coupling and Energy Squeezing Using a Microwave Waveguide," *Phys. Rev. Lett.,* Vol. 100, no. 3, 033903, pp. 1-4, Jan. 2008.

[6] W. Rotman, "Plasma simulation by artificial dielectrics and parallel-plate media," *IRE Trans. Antennas Propag*., Vol. 10, no. 1, pp. 82-95, Jan. 1962.

[7] A. Alu and N. Engheta, "Antenna matching in ε-near-zero metamaterial channels," presented at the *IEEE International Workshop on Antenna Technology, 2009. iWAT*, Los Angeles California, March 2-4, 2009, pp. 1 – 4.

[8] B. Edwards, A. Alù, M. G. Silveirinha, and N. Engheta, "Reflectionless Sharp Bends and Corners in Waveguides Using Epsilon-Near-Zero Effects," *J. Appl. Phys.*, Vol. 105, no. 4, 044905, pp. 1-4, Feb.2009.

[9] A. Alu and N. Engheta, "Dielectric Sensing in ε-Near-Zero Narrow Waveguide Channels," *Phys. Rev. B.,* Vol. 78, no. 4, 045102, pp. 1-5, Jul. 2008.

[10] R. Liu, Q. Cheng, T. Hand, J. J. Mock, T. J. Cui, S. A. Cummer, and D. R. Smith, "Experimental Demonstration of Electromagnetic Tunneling Through an Epsilon-Near-Zero Metamaterial at Microwave Frequencies," *Phys. Rev. Lett.,* Vol. 100, no. 1, 023903, pp. 1-4, Jan. 2008.

[11] Ansoft HFSS simulator, v. 11.